

# Polymorphism of Scyllo-Inositol: Joining Crystal Structure Prediction with Experiment to Elucidate the Structures of Two Polymorphs

Graeme M. Day,<sup>\*,†</sup> Jacco van de Streek,<sup>‡</sup> Arnaud Bonnet,<sup>†</sup> Jonathan C. Burley,<sup>§</sup> William Jones,<sup>†</sup> and W. D. Sam Motherwell<sup>‡</sup>

The Pfizer Institute for Pharmaceutical Materials Science, Department of Chemistry, University of Cambridge, Lensfield Road, Cambridge, CB2 1EW, United Kingdom, The Cambridge Crystallographic Data Centre, 12 Union Road, Cambridge, CB2 1EZ, United Kingdom, and Department of Chemistry, University of Cambridge, Lensfield Road, Cambridge, CB2 1EW, United Kingdom

Received March 31, 2006; Revised Manuscript Received July 19, 2006

**ABSTRACT:** We report on the crystal structures of two polymorphs of scyllo-inositol. Crystallization of this inositol initially failed to yield a single crystal suitable for structure solution, so a computational prediction of the low-energy forms was performed in parallel with the crystallization experiments. When a single crystal was finally grown, its structure failed to explain the powder X-ray diffraction pattern of the bulk material, which seemed to show a mixture of polymorphs. With the aid of the lowest-energy predicted crystal structure from a lattice energy search and the DASH program for structure solution from powder data, we propose the structure of the second polymorph. The combined use of single-crystal structure solution, structure solution from powder diffraction data, and a lattice energy search for possible structures, which was necessary for the elucidation of the second polymorph of scyllo-inositol, demonstrates the synergy between experimental and computational studies of molecular organic materials.

## Introduction

Polymorphism of pharmaceutical compounds is of vital importance in industry, for both the establishment of patents and control of physical properties of the delivered drug.<sup>1</sup> The identification and characterization of all crystalline forms accessible under ambient conditions is an expensive and lengthy experimental procedure and is often hampered by the difficulty of obtaining single crystals suitable for routine structure determination by X-ray analysis. In practice, the existence of unstable polymorphs is often detected only by powder X-ray diffraction (PXRD), and in recent years, reliable techniques have been devised to determine crystal structures from PXRD in direct space.<sup>2,3</sup> However, difficulties in structure determination from powder diffraction data can arise because a powder sample may not be pure and/or may contain a minor component of another polymorph. We report here such a case for the molecule scyllo-inositol, the difficulty being encountered during a broader investigation of the hydrogen-bonding patterns in inositols and related isomeric compounds; inositols are sometimes used as excipients in pharmaceutical tablets and scyllo-inositol is a potential new therapeutic for Alzheimer's disease.<sup>4</sup> Scyllo-inositol, with the all-equatorial hydroxyl configuration (Figure 1), has no previously reported crystal structure, so we sought its structure to compare with the other inositols. Here, we report our experiences in solving the crystal structures of two scyllo-inositol polymorphs; the characterization of this dimorphic system could be completed only through a combination of experimental and computational techniques.

Chronologically, our experiences were as follows. Crystallization of scyllo-inositol to obtain a crystal suitable for single crystal XRD analysis was initially unsuccessful, so we attempted structure solution from the powder pattern. However, the powder

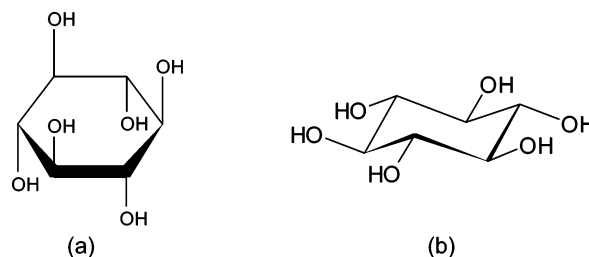


**Figure 1.** Scyllo-inositol (a) Haworth projection formula; (b) chair structure.

diffraction pattern could not be indexed, which is a prerequisite for structure solution from powder data. Crystal structure prediction has long promised itself as a tool to aid in resolving crystal structures when difficulties prevent direct solution from experimental data;<sup>5</sup> such predictions have been used successfully to help determine crystal structures without the need to index the powder pattern.<sup>5-8</sup> We decided to put current methods to the test in attempting the prediction of the low-energy crystal structures of scyllo-inositol, hoping that a knowledge of possible low-energy structures would help characterize the crystalline system.

As these calculations were proceeding, we finally obtained a single crystal of scyllo-inositol by recrystallization from aqueous solution, leading to a triclinic structure with unit cell data as in Table 1. In comparing the observed powder pattern to that simulated from the single-crystal structure (Figure 2b), we noted sufficient differences to suspect that we were studying a polymorphic system: chemical purity of the powder sample had been confirmed by elemental analysis, so we took the presence of additional reflections seen in the measured PXRD pattern as evidence of further crystal forms of scyllo-inositol. Indeed, in 1912, Müller<sup>9</sup> reported limited crystal parameters (ratios of unit-cell parameters) for a monoclinic form (Table 1); several attempts by us to grow single crystals of the second form were unsuccessful. Neither could we obtain a pure powder sample, i.e., one containing no evidence of the triclinic form. Aided by

\* To whom correspondence should be addressed. Fax: +44 (0)1223 336362. E-mail: gmd27@cam.ac.uk.

<sup>†</sup> The Pfizer Institute for Pharmaceutical Materials Science, Department of Chemistry, University of Cambridge.

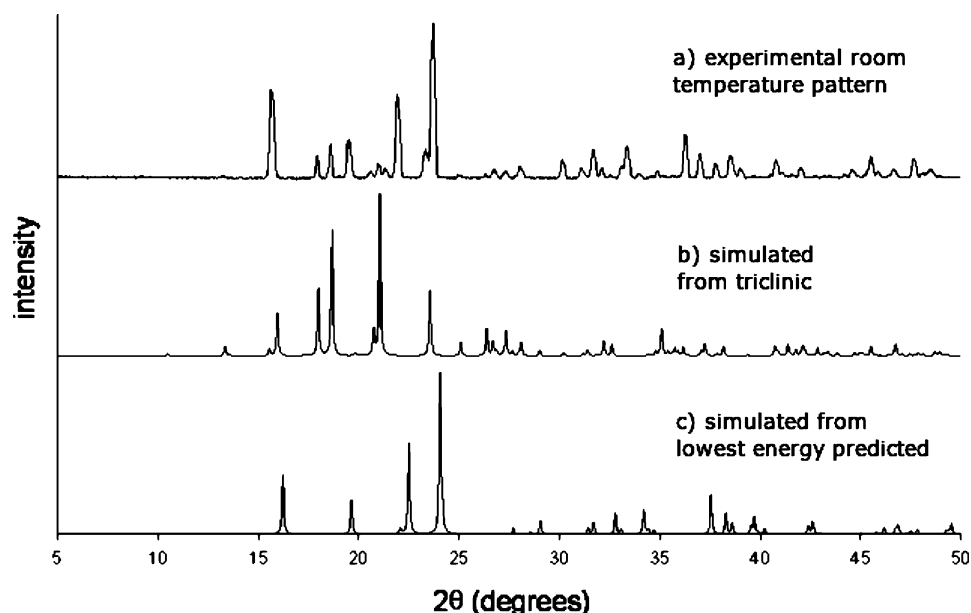
<sup>‡</sup> The Cambridge Crystallographic Data Centre.

<sup>§</sup> Department of Chemistry, University of Cambridge.

**Table 1.** Summary of Results Obtained from Single-Crystal X-ray Analysis at 180 K (triclinic form), the Global Energy Minimum of the Crystal Structure Prediction Study, and the Final Structure Refined from Powder Diffraction Data (monoclinic, DASH) Obtained at Room Temperature

crystal params	single-crystal X-ray <sup>a</sup>	global minimum predicted structure	refined structure using powder X-ray data	Müller <sup>9</sup>
cryst syst	triclinic	monoclinic	monoclinic	monoclinic
space Group	$P\bar{1}$	$P2_1/c$	$P2_1/c$	
<i>a</i> (Å)	6.7176(2)	5.00	5.0943	
<i>b</i> (Å)	6.7638(2)	6.44	6.6459	
<i>c</i> (Å)	8.6217(3)	11.42	11.9617	
<i>a</i> : <i>b</i> : <i>c</i>	0.779:0.785:1	0.776:1:1.773	0.766:1:1.800	0.765:1: 1.794
$\alpha$ (deg)	95.355(1)	90	90	90
$\beta$ (deg)	99.686(1)	115.4	116.9617	117
$\gamma$ (deg)	98.879(1)	90	90	90
<i>V</i> (Å <sup>3</sup> )	378.66(2)	332.0	360.84	
<i>Z</i>	2	2	2	

<sup>a</sup> Data for single-crystal XRD determination:  $T = 180(2)$  K,  $\mu(\text{Mo-K}\alpha) = 0.143 \text{ mm}^{-1}$ ,  $\rho_{\text{calcd}} = 1.540 \text{ g cm}^{-3}$ ,  $\lambda = 0.71073 \text{ \AA}$ ,  $\theta$  range =  $3.58\text{--}27.43^\circ$ . Final residuals for 128 parameters were  $R_1 = 0.0335$ ,  $wR_2 = 0.0873$  for  $I > 2\sigma(I)$ , and  $R_1 = 0.0390$ ,  $wR_2 = 0.0909$  for all 1717 data.

**Figure 2.** PXRD pattern for (a) the as-received sample of scyllo-inositol and simulated PXRD patterns for (b) the triclinic structure obtained by single-crystal X-ray analysis and (c) from the lowest-energy predicted crystal structure (wavelength = 1.54056 Å).

the results of the crystal structure prediction calculations, we set out to solve the structure of the second form from the powder diffraction data of the mixed sample, using the program DASH.

### Methods

**Experimental.** Scyllo-inositol ( $\geq 98\%$ ) was obtained from Sigma as a white crystalline solid and its purity confirmed by <sup>13</sup>C solution NMR. Elemental analysis gave C, 40.08; H, 6.63; O, 53.29 (calcd: C, 40.00; H, 6.7; O, 53.29). The melting point onset, determined by DSC at a heating rate of  $10 \text{ K min}^{-1}$ , was 628 K. The analytical results indicated that the sample was pure; the PXRD reflections were sharp, indicating high crystallinity. A sample of scyllo-inositol was recrystallized as single crystals by vapor diffusion of methanol into a concentrated aqueous solution.

Single-crystal X-ray diffraction data was collected at 180(2) K with a Nonius Kappa CCD diffractometer using MoK $\alpha$  radiation ( $\lambda = 0.71073$ ) and equipped with an Oxford Cryostream system. The structure was solved by direct methods and refined on  $F^2$  against all data using *SHELXL-97* (University of Göttingen, Germany, 1997). All non-hydrogen atoms were refined with anisotropic displacement parameters. The OH hydrogen atoms were located in difference Fourier maps and refined isotropically. All other hydrogen atoms were placed geometrically and were allowed to ride during subsequent refinement.

PXRD scans for crystal structure determination were collected on a Philips X'Pert Pro diffractometer at 40 kV and 40 mA with an X'Celerator RTMS detector, with monochromatic X-ray CuK $\alpha_1$  radi-

ation ( $\lambda = 1.54056 \text{ \AA}$ ) generated with an incident focusing beam Johansson monochromator using a Ge(111) crystal. Samples were prepared for collection by filling a 0.5 mm diameter borosilicate glass capillary. The spinning capillary was analyzed at ambient temperature between 5 and  $80^\circ 2\theta$  with a step size of  $0.017^\circ 2\theta$ . Low-temperature (180 K) PXRD data were collected using a Stoe Stadi-P diffractometer with monochromatic CoK $\alpha_1$  radiation operating in Debye–Scherrer geometry. The sample was contained in a 0.7 mm diameter borosilicate glass capillary. Temperature control was achieved using an Oxford Cryostream system.

**Computational Methods.** We undertook the computational search for the low-energy crystal forms of scyllo-inositol before the structure of either polymorph was known. The following methodology was used to give the greatest chance of locating the best structures within the constraints of time and computational resources that could be dedicated to the calculations.

The Monte Carlo simulated annealing algorithm, as implemented in the Polymorph Predictor module of Cerius<sup>2,10</sup> was used to generate low-energy crystal structures within the six most likely space groups for this molecule, all with a single molecule in the asymmetric unit ( $Z' = 1$ )<sup>11</sup>. The two main steps in generating hypothetical structures are simulated annealing to generate loosely packed trial structures, followed by energy minimization to refine these starting points, resulting in a set of  $T = 0 \text{ K}$  crystal structures. The final energy minimizations were performed using the COMPASS<sup>12</sup> force field, which allows full molecular flexibility and has realistically reproduced the properties of inositols in molecular dynamics simulations.<sup>13</sup> Electrostatic interactions

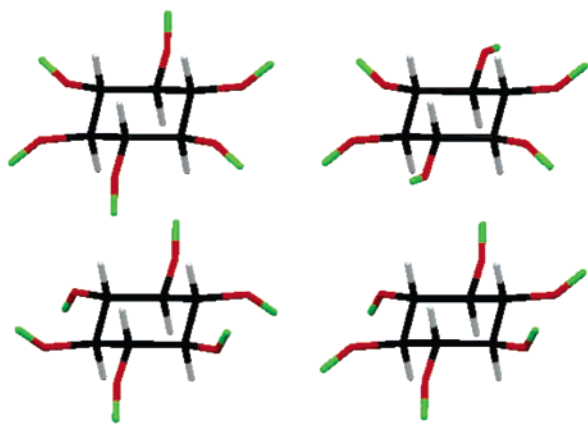


**Figure 3.** Starting conformations used in the crystal structure search. Hydroxyl hydrogen atoms are highlighted in green to emphasize the differences between conformations.

were modeled with atomic charges fitted to the electrostatic potential calculated from a DFT (Dmol3,<sup>14</sup> VWN–BP/DNP) wave function around the isolated molecule.<sup>15</sup> All atom–atom interactions were summed to a 20 Å direct-space cutoff, except for electrostatic interactions, which were calculated using Ewald summation. All crystal structures were energy minimized with no constraints on the molecular geometry in the final step of the calculations, allowing reorientation of the hydroxyl groups to optimize hydrogen bonding. However, as the simulated annealing algorithm involves an initial search using a rigid molecular model, starting molecular geometries had to be carefully chosen to explore the packing of all important conformations (see below).

The C<sub>6</sub> ring is in the chair conformation in all known inositol crystal structures, so we used a chair conformation in all searches and considered only the hydroxyl orientations as important degrees of freedom. The computing time was not available to start searches from all possible combinations of the six hydroxyl group orientations, so we used a smaller set of starting geometries, chosen to give the best chance of sampling all important conformations during energy minimization. Following analysis of hydroxyl orientations in crystal structures of other inositols, conformational energy calculations, and short tests of the simulated annealing, we chose four molecular models (Figure 3) as starting points for the search. Instead of minimum-energy conformations, which tend to remain fixed because of the barriers involved with reorientation of the hydroxyl groups, we started with higher-energy hydroxyl orientations that were free to reorient to the most favorable geometry for hydrogen bonding (further details on the choice of starting molecular geometries are given in the Supporting Information).

Structure solution from powder data was performed using the DASH software,<sup>16</sup> which uses a simulated annealing algorithm in a global optimization approach to structure solution from powder data. As the measured powder pattern could not be indexed, the unit cell and space group symmetry were taken from the most promising low-energy predicted crystal structure, as described in more detail in the following section. The GSAS program<sup>17</sup> was used for final two-phase Rietveld refinement.

## Results

The small colorless crystals of scyllo-inositol had a melting point onset of 628 K by DSC at a heating rate of 10 K min<sup>−1</sup>.

**Table 2.** Unit Cells and Relative Energies of the Five Most Stable Predicted Crystal Structures of Scyllo-Inositol

relative energy (kJ mol <sup>−1</sup> )	space group	<i>a</i> (Å)	<i>b</i> (Å)	<i>c</i> (Å)	$\alpha$ (deg)	$\beta$ (deg)	$\gamma$ (deg)	$\rho$ (g cm <sup>−3</sup> )
0	<i>P</i> <sub>2</sub> <sub>1</sub> / <i>c</i> ( <i>Z'</i> = 1/2)	5.001	6.437	11.420	90	115.4	90	1.802
4.30	<i>R</i> <sup>3</sup> ( <i>Z'</i> = 1/2)	12.012	12.012	4.270	90	90	120	1.682
10.81	<i>C</i> 2/ <i>c</i> ( <i>Z'</i> = 1)	21.484	6.291	11.480	90	108.9	90	1.630
11.27	<i>C</i> 2/ <i>c</i> ( <i>Z'</i> = 1)	20.172	6.352	11.427	90	97.4	90	1.648
11.97	<i>P</i> <sub>2</sub> <sub>1</sub> / <i>c</i> ( <i>Z'</i> = 1)	9.565	6.289	11.486	90	97.8	90	1.748
	Energy-Minimized Triclinic Crystal Structure							
14.93	<i>P</i> <sup>1</sup> ( <i>Z'</i> = 2 × 1/2)	6.448	6.856	8.159	92.8	104.7	94.5	1.725

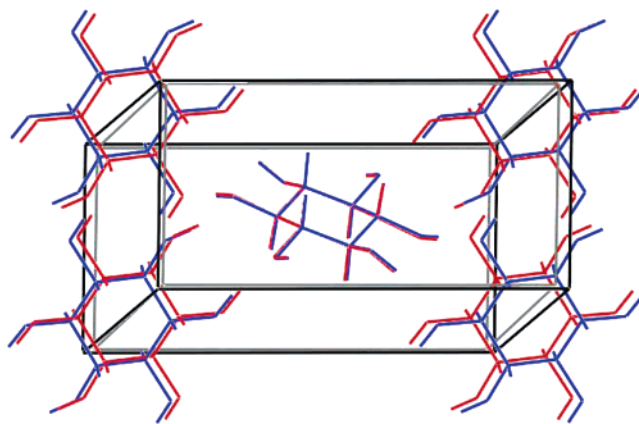


**Figure 4.** Overlay of the lowest-energy predicted crystal structure (red, with gray cell axes) and lowest  $\chi^2$  DASH solution from the PXRD data (blue with black cell axes).

Unit-cell parameters of the triclinic (*P*<sup>1</sup>, *Z* = 2) crystal structure are reported in Table 1. The unit cell contains two independent molecules, each sitting on an inversion center. Hence, the asymmetric unit consists of two half-molecules.

The experimental powder diffraction pattern did not match the powder diffraction pattern simulated from the single-crystal structure of the triclinic form (Figure 2): the strongest reflection (21.0° 2 $\theta$ ) from the simulated pattern was very weak in the experimental pattern and the three strongest reflections (15.7, 21.9, and 23.7° 2 $\theta$ ) in the experimental pattern were absent from the simulated pattern. It became clear that the experimental pattern should be attributed to a mixture of a small amount of the triclinic crystal and a larger component of a second polymorph, the crystal structure of which we set out to solve from the powder diffraction data.

The first step was to index the pattern, i.e., determine the unit cell, which relies on accurate determination of the positions of about 20 reflections that can be assigned to the new polymorph. Unfortunately, indexing was not successful because (i) despite being the minor component, the known triclinic polymorph gave a large number of reflections; (ii) the triclinic cell was measured at 180 K and the experimental PXRD pattern at room temperature, and the resulting peak shifts made it impossible to assign peaks unambiguously.<sup>18</sup> Unable to index the pattern for structure solution from powder diffraction data, we compared the experimental pattern to the simulated PXRD for the lowest-energy predicted crystal structures.

Compared to many small molecules, the crystal structure prediction calculations showed surprisingly few predicted structures within a few kilojoules per mole of the global minimum predicted structure; the two most stable were separated from the rest by 6.5 kJ/mol, an unusually large energy gap in crystal structure prediction studies.<sup>19</sup> The triclinic form was not present in our list of predicted structures; we would have had to perform the simulated annealing with two independent molecules to find the unusual packing with two-half molecules

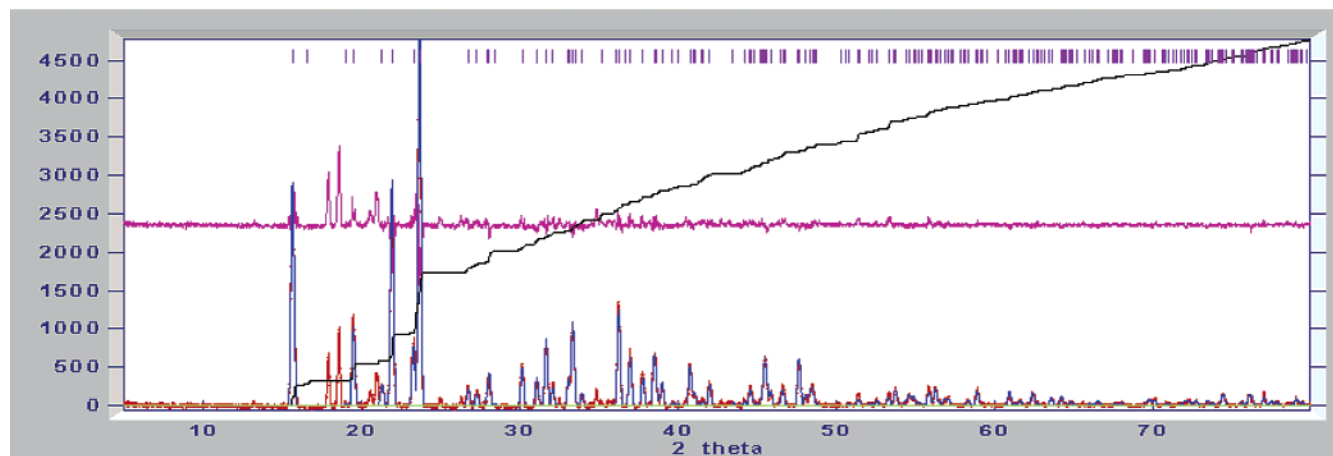


**Figure 5.** Calculated (blue), observed (red), and difference (magenta) profile. Tick marks are shown in green, the cumulative  $\chi^2$  is shown in black. Some discrepancies due to the presence of the triclinic polymorph are clearly visible.

in the asymmetric unit. For comparison with the predicted structures, we energy-minimized the triclinic crystal structure with the same force field as that used in our predictions (Table 2). The force field assigned a high relative energy to the triclinic crystal structure, nearly 15 kJ/mol above the global minimum of our predictions. This energy difference seems unreasonable,<sup>20</sup> so we recognize the limitations of the methodology and force field for evaluating the relative stability of the real and computer-generated crystal structures. Nevertheless, we proceeded with our examination of the low-energy predictions; despite uncertainties in the relative stability of the computer-generated structures, the predicted structures could still provide a useful starting point for explaining the observed powder pattern.

The small number of low-energy structures simplified the comparison of predicted structures to the unexplained reflections in the measured PXRD pattern; even with large errors in the calculated energies, we could examine a small number of the predicted crystal structures, ruling out the rest as energetically unreasonable. We started by considering only the five most stable predicted structures (Table 2) to see if we could find one that would help explain the observed powder pattern. Only one pattern (Figure 2c), corresponding to the lowest-energy predicted crystal structure, gave a good match for the five strongest observed reflections that are not associated with the triclinic form.

Assuming that this predicted crystal structure corresponded to the second polymorph, we now had the space group ( $P2_1/c$ ) and an estimate of the unit-cell parameters to within about  $\pm 3$ –5% (Table 1), the accuracy expected from force-field-based lattice-energy minimization. However, small inaccuracies in the unit-cell parameters of the predicted crystal structure, combined with the problems with the PXRD pattern mentioned above, still made it impossible to assign any reflections other than the strongest five to the second polymorph. Therefore, a computer program was written to perform a grid search to find values for  $a$ ,  $b$ ,  $c$ ,  $\beta$ , and the zero-point error (i.e., the instrumental error at  $2\theta = 0^\circ$ ) in the neighborhood of those from the predicted crystal structure that gave the best match to the five strongest reflections. The remaining steps in the structure solution from the powder data—Pawley refinement, simulated annealing, and rigid-body Rietveld refinement—were then performed using the DASH program.<sup>16</sup> With the best unit-cell parameters from the grid search and the space group  $P2_1/c$  from the predicted crystal structure, the Pawley refinement progressed smoothly to a Pawley  $\chi^2$  value of 10.39. The rather large value is caused, of

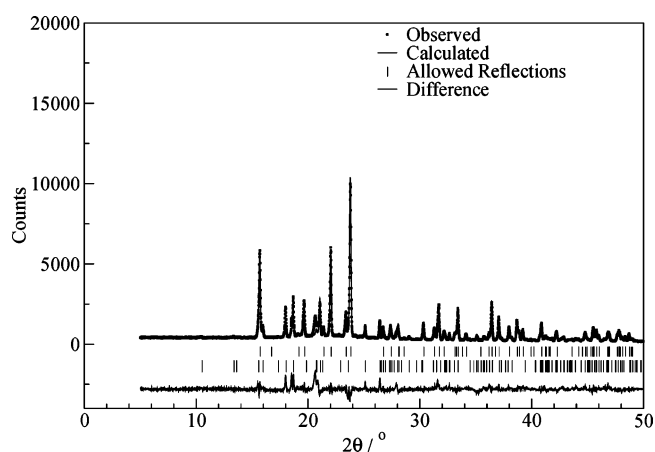


**Figure 6.** Two-phase Rietveld refinement of the mixture of two scyllo-inositol polymorphs. The lower set of tick marks corresponds to the triclinic polymorph and the upper tick marks correspond to the monoclinic polymorph. Some discrepancies due to the presence of an unknown impurity are clearly visible in the difference pattern (see text).

course, by the presence of two medium strong reflections from the triclinic polymorph.

For structure solution, we used a molecular model with a rigid geometry obtained from the predicted crystal structure, constrained to sit on a center of symmetry at  $[0, 0, 0]$ . There are no flexible torsion angles besides those describing the hydroxyl orientations, leaving only three rotational degrees of freedom to be determined. Within seconds, 10 nearly identical solutions had been obtained, differing only in the positions of the hydrogen atoms. The solution with the lowest  $\chi^2$  value corresponded to the predicted crystal structure (these are overlaid in Figure 4) and was the only arrangement in which every O—H $\cdots$ O hydrogen bond contained one hydrogen atom with sensible geometry.

Although the fit (Figure 5) is convincing evidence that we have a good model of the monoclinic polymorph, we performed a two-phase Rietveld refinement as a final confirmation. We found that although simultaneous refinement of all structural parameters of the two polymorphs was problematic, we were able to refine atomic displacement parameters and lattice parameters of the triclinic phase, along with all parameters of the monoclinic phase (i.e., including molecular geometry; Figure 6). Suitable restraints were imposed on molecular bond lengths and angles, based on the results from the single-crystal study. The molecular position, orientation, and internal torsion angles

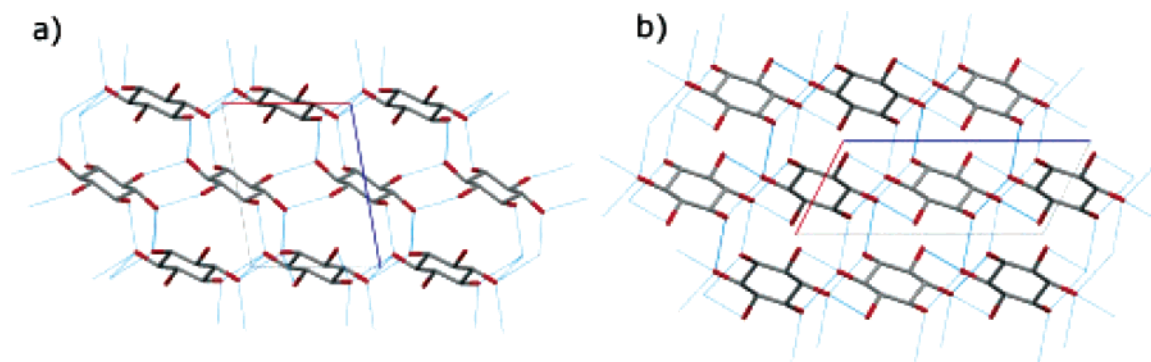


**Figure 7.** (a) Packing diagram for the  $P\bar{1}$  structure (single-crystal analysis). (b) Packing diagram for the  $P2_1/c$  structure (powder analysis). Hydrogen atoms are omitted for clarity. Hydrogen bonds are shown as dotted blue lines.

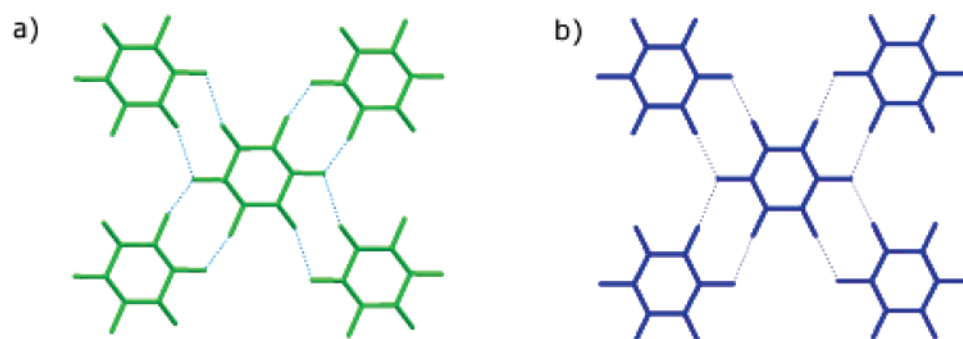


**Figure 8.**  $P\bar{1}$  structure showing sheets of (a) all A (green) and (b) all B (blue) molecules in almost identical configurations. Each molecule is linked to four others by pairs of strong hydrogen bonds. Hydrogen bonds perpendicular to the sheet have been omitted for clarity.

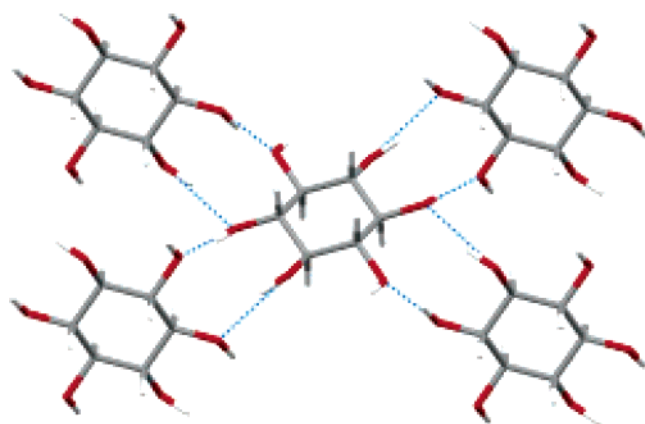


**Figure 9.**  $P2_1/c$  structure showing hydrogen-bonded neighbors in the sheet perpendicular to a. Hydrogen bonds perpendicular to the sheet are omitted. Every molecule is linked by a pair of hydrogen bonds to each neighbor.

were allowed to refine freely where appropriate and allowed by symmetry. The cell parameters (Table 1) are all 2–5% larger than those of the predicted crystal structure. These differences between lattice-energy-minimized and observed structures are of the same magnitude as for other crystals of small organic molecules, and the volume difference (8%) is in line with typical thermal expansion between  $T = 0$  K and room temperature. The two-phase refinement from the powder pattern may have been possible starting directly from the single-crystal triclinic structure and the predicted monoclinic crystal structure. The intermediate simulated annealing in the DASH step provided a check that no other packing with the same intensities existed for this unit cell, giving extra confidence in the final solution.

The refinement gave a 3.6:1 (monoclinic:triclinic) molar ratio of the two polymorphs in the bulk sample. Although we are happy that the two-phase refinement confirms the correctness of the model of the monoclinic polymorph, there are several reflections from an unidentified phase that result in relatively poor goodness of fit ( $R_{wp} = 15.36\%$ ,  $R_p = 10.50\%$ ,  $\chi^2 = 14.20$ ,  $R_{Bragg} = 17.52\%$ ). As yet, we have not identified the nature of this phase; the fact that the elemental analysis was unaffected suggests either a third polymorph or another inositol isomer.

**Comparison of the Polymorph Structures.** The packing diagrams for the two structures are shown in Figure 7; we chose a view that shows a visual similarity with regard to the general orientation and position of the molecules. There are sheets of molecules in both crystal structures, here seen as horizontal sections through the crystal, which in fact have considerable hydrogen-bonding similarity, as discussed below. Scyllo-inositol has the highest molecular symmetry,  $D_{3d}$ , of the reported isomers of inositol<sup>21</sup> and it is interesting that this molecular symmetry is comparatively rare in the CSD. A survey<sup>22</sup> reported that there were only 89 molecules with symmetry  $D_{3d}$  in the CSD, of which only one was in a general position in the cell; all others were in special positions, and 48% occupied a center of symmetry. It was therefore unsurprising that molecules in both of the scyllo-inositol polymorphs sit on inversion centers; the  $P\bar{1}$  structure has two independent molecules occupying two different crystallographic centers of symmetry, the  $P2_1/c$  structure has only one independent molecule.

**Hydrogen-Bonded Neighbors.** Comparison of the hydrogen bonding (here defined as  $O\cdots O$  contacts  $< 3.04$  Å) in the two polymorphs reveals a basic similarity with regard to the view from one molecule. In the triclinic form, both molecules in the asymmetric unit, A and B, have a similar immediate hydrogen-bonded environment; each molecule is linked to eight neighboring molecules by a total of 12 hydrogen bonds, with the various

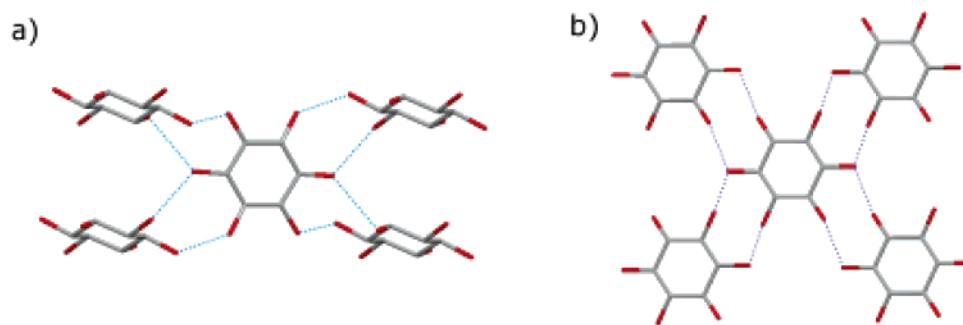


**Figure 10.** Comparison of the sheets of double-linked molecules in (a) the  $P2_1/c$  structure and (b) the  $P\bar{1}$  structure. The central molecule is viewed perpendicular to its mean plane.

OH groups having different numbers of associated hydrogen bonds. We find a similar arrangement in the  $P2_1/c$  structure, with some difference in orientation of the molecules that is discussed below.

**Similar Sheets of Hydrogen Bonds.** Despite the apparent dissimilarity in hydrogen-bond counts per OH group, we find similar features of the total packing. In  $P\bar{1}$  (Figure 7a), we see horizontal sheets of molecules perpendicular to  $c$  that are all of the same type and alternate in sheets of all A and all B. There are similar sheets in the  $P2_1/c$  structure (Figure 7b), seen in the horizontal sections perpendicular to  $a$ .

The bonding within a sheet (Figure 8) intuitively seems to be a mechanically stable arrangement, as each molecule is linked by pairs of hydrogen bonds to four immediate neighbors. These pairs of hydrogen bonds are symmetrical, using the crystal centers of symmetry, with O...O distances of 2.713, 2.909, 2.694, and 2.742 Å. There are four hydrogen bonds per molecule approximately perpendicular to the sheet linking to the next sheet in the  $c$ -direction, giving the complete crystal structure.

The structure of the  $P2_1/c$  polymorph has just one independent molecule but shows a similar sheet structure, arranged perpendicular to the  $a$ -direction (Figure 9). Thus we may describe both polymorph structures as strongly double-linked molecular sheets, with each molecule linked by a set of four single hydrogen-bond links to adjacent sheets. If we compare the geometry of the sheets, see Figure 10, we see that the  $P2_1/c$  structure has the neighbors in the sheets at a greater angle to the mean plane of the reference molecule, giving a buckled sheet, whereas the  $P\bar{1}$  structure shows a more planar sheet. One could imagine that conversion of one polymorph to the other might be feasible with little movement of the molecular centers and a change of orientation of the molecule to the plane of the sheet. We do not have any experimental evidence at present as to which structure is the more stable polymorph; repeating the PXRD measurement on the same sample after 5 months showed no perceptible change.

### Conclusions

The crystal structures of two polymorphs of scyllo-inositol have been determined, one from single-crystal X-ray diffraction and the second by using a low-energy computer-generated crystal structure as a starting point for structure solution from powder data using DASH. Individually, the methods used to study this molecular organic material could not have fully characterized the crystal structures of this dimorphic molecule. Although single-crystal structure solution is the preferred method of accurately determining the three-dimensional structure of a crystal, the inability to crystallize suitable single crystals should no longer be a barrier to determining the structure of a crystal.

Methods for solving structures from powder diffraction data have become reliable in recent years and computational methods of proposing the most likely crystal structures of a given molecule have developed into useful tools for the materials chemist.

The case of scyllo-inositol was complicated by the presence of a polymorphic impurity (i.e., the triclinic polymorph), which can prevent structure solution from powder data. However, the single-crystal solution of one polymorph allowed for identification of diffraction reflections belonging to this form, and the success of the computational search provided a high enough quality starting point for refinement to the remaining reflections. This experience of a combined approach to structure determination from an otherwise intractable PXRD, containing polymorphic impurities, demonstrates a valuable application of computational methods in crystal structure prediction and structure solution from powder diffraction data.

**Acknowledgment.** We thank the Pfizer Institute for Pharmaceutical Materials Science for funding and are grateful to Dr. John Davies (Department of Chemistry, University of Cambridge) for single-crystal data collection and structure solution. J.C.B. thanks Jesus College, Cambridge, for the award of a Junior Research Fellowship.

**Supporting Information Available:** Crystallographic information files (CIFs) of the two polymorphs of scyllo-inositol; computational details and description of the choice of starting molecular conformations (PDF). This material is available free of charge via the Internet at <http://pubs.acs.org>.

### References

- (1) Brittain, H. G. *Polymorphism in Pharmaceutical Solids: Drugs and the Pharmaceutical Sciences*; Marcel Dekker: New York, 1999; Vol. 95.
- (2) Harris, K. D. M.; Tremayne, M.; Kariuki, M. *Angew. Chem. Int. Ed.* **2001**, *40*, 1626–1651.
- (3) Shankland, K.; Florence, A. J.; Shankland, N.; David, W. I. F.; Johnston, A.; Markvardsen, A. J.; Steele, G.; Cosgrove, S. D. *Am. Pharm. Rev.* **2004**, *7*, 80–86.
- (4) McLaurin, J.; Kierstead, M. E.; Brown, M. E.; Hawkes, C. A.; Lambermon, M. H.; Phinney, A. L.; Darabie, A. A.; Cousins, J. E.; French, J. E.; Lan, M. F.; Chen, F.; Wong, S. S. N.; Mount, H. T. J.; Fraser, P. E.; Westaway, D.; St. George-Hyslop, P. *Nat. Med.* **2006**, *12*, 801–808.
- (5) Karfunkel, H. R.; Wu, Z. J.; Burkhard, A.; Rihs, G.; Sinnreich, D.; Buerger, H. M.; Stanek, J. *Acta Crystallogr., Sect. B* **1996**, *52*, 555–561.
- (6) Bond, A. D.; Jones, W. *Acta Crystallogr., Sect. B* **2002**, *58*, 233–242.
- (7) McArdle, P.; Gilligan, K.; Cunningham, D.; Dark, R.; Mahon, M. *CrystEngComm* **2004**, *6*, 303–309.
- (8) Schmidt, M. U.; Ermrich, M.; Dinnebier, R. E. *Acta Crystallogr., Sect. B* **2005**, *61*, 37–45.
- (9) Müller, H. *J. Chem. Soc.* **1912**, *101*, 2383–2410.
- (10) *Cerius2*, version 4.6; Accelrys Inc.: San Diego, CA, 2001.

- (11) The space groups  $P1$ ,  $P2_1/c$ ,  $P\bar{1}$ ,  $P2_1$ ,  $P2_12_12_1$ , and  $C2/c$  were searched; approximately 80% of known crystal structures of organic molecules occur in these space groups and, as is clear from the list of final structures, they also allow some sampling of higher-symmetry space groups. Furthermore,  $Z' = 0.5$  crystal structures are located in these searches, when the molecule finds a special position during energy minimization.
- (12) Sun, H. J. *Phys. Chem.* **1998**, *102*, 7338.
- (13) Watt, S. W.; Chisholm, J. A.; Jones, W.; Motherwell, W. D. S. *J. Chem. Phys.* **2005**, *121*, 9565–9573.
- (14) Delley, B. J. *Chem. Phys.* **1990**, *92*, 508–517.
- (15) For the fitting of atomic charges, the molecular geometry was energy minimized with  $D_{3h}$  symmetry constraints, with OH bonds kept trans to the adjacent CH bonds, preventing intramolecular hydrogen bonding.
- (16) David, W. I. F.; Shankland, K.; van de Streek, J.; Pidcock, E.; Motherwell, W. D. S. *DASH*, version 3.0; Cambridge Crystallographic Data Centre: Cambridge, U.K..
- (17) Larson, A. C.; Von Dreele, R. B. *General Structure Analysis System (GSAS)*; Los Alamos National Laboratory Report LAUR 86-748; Los Alamos National Laboratory: Los Alamos, NM, 2000.
- (18) We did recollect the powder pattern at 180 K for final two-phase refinement, but the resulting pattern was still not suitable for determining the unit cell of the second polymorph.
- (19) Day, G. M.; Chisholm, J.; Shan, N.; Motherwell, W. D. S.; Jones, W. *Cryst. Growth Des.* **2004**, *4*, 1327–1340.
- (20) A rule of thumb for the maximum energy difference between polymorphs is often quoted as 10 kJ/mol.
- (21) CSD reference codes of the other inositols are EPINOS (epi-inositol), FOPKOK (L-chiro-inositol), MUINOS (muco-inositol), MYINOL (myo-inositol), and YEPNOW (neo-inositol).
- (22) Pidcock, E.; Motherwell, W. D. S.; Cole, J. C. *Acta Crystallogr., Sect. B* **2003**, *59*, 634–640.

CG060179A